Oecologia (2003) 134:37–45
DOI 10.1007/s00442-002-1080-8

ECOPHYSIOLOGY

Shelley A. James · Frederick C. Meinzer · Guillermo Goldstein · David Woodruff · Timothy Jones · Teresa Restom · Monica Mejia · Michael Clearwater · Paula Campanello

Axial and radial water transport and internal water storage in tropical forest canopy trees

Received: 8 March 2002 / Accepted: 3 September 2002 / Published online: 18 October 2002

Abstract Heat and stable isotope tracers were used to study axial and radial water transport in relation to sapwood anatomical characteristics and internal water storage in four canopy tree species of a seasonally dry tropical forest in Panama. Anatomical characteristics of the wood and radial profiles of sap flow were measured at the base, upper trunk, and crown of a single individual of *Anacardium excelsum*, *Ficus insipida*, *Schefflera morototoni*, and *Cordia alliodora* during two consecutive dry seasons. Vessel lumen diameter and vessel density did not exhibit a consistent trend axially from the base of the stem to the base of the crown. However, lumen diameter decreased sharply from the base of the crown to the terminal branches. The ratio of vessel lumen area to sapwood cross-sectional area was consistently higher at the base of the crown than at the base of the trunk in *A. excelsum*, *F. insipida* and *C. alliodora*, but no axial trend was apparent in *S. morototoni*. Radial profiles of the preceding wood anatomical characteristics varied according to species and the height at which the wood samples were obtained. Radial profiles of sap flux density measured with thermal dissipation sensors of variable length near the base of the crown were highly correlated with radial profiles of specific hydraulic conductivity (k_s) calculated from xylem anatomical characteristics. The relationship between sap flux density and k_s was species-independent. Deuterium oxide (D_2O) injected into the base of the trunk of the four study trees was detected in the water transpired from the upper crown after only 1 day in the 26-m-tall *C. alliodora* tree, 2 days in the 28-m-tall *F. insipida* tree, 3 days in the 38-m-tall *A. excelsum* tree, and 5 days in the 22-m-tall *S. morototoni* tree. Radial transport of injected D_2O was detected in *A. excelsum*, *F. insipida* and *S. morototoni*, but not *C. alliodora*. The rate of axial D_2O transport, a surrogate for maximum sap velocity, was positively correlated with the predicted sapwood k_s and with tree height normalized by the relative diurnal water storage capacity. Residence times for the disappearance of the D_2O tracer in transpired water ranged from 2 days in *C. alliodora* to 22 days in *A. excelsum* and were positively correlated with a normalized index of diurnal water storage capacity. Capacitive exchange of water between stem storage compartments and the transpiration stream thus had a profound influence on apparent rates of axial water transport, the magnitude of radial water movement, and the retention time in the tree of water taken up by the roots. The inverse relationship between internal water exchange capacity and k_s was consistent with a trade-off contributing to stability of leaf water status through highly efficient water transport at one extreme and release of stored water at the other extreme.

Keywords Capacitance · D/H ratios · Hydraulic architecture · Sap flow · Xylem anatomy

S.A. James · G. Goldstein · T. Restom · T. Jones · M. Mejia
Department of Botany, University of Hawaii, St John 101, Honolulu, HI 96822, USA

F.C. Meinzer (✉)
USDA Forest Service Forestry Sciences Laboratory, 3200 SW Jefferson Way, Corvallis, OR 97331, USA
e-mail: fmeinzer@fs.fed.us
Tel.: +1-541-7587798
Fax: +1-541-7587760

D. Woodruff
Department of Forest Science, Oregon State University, Corvallis, OR 97331, USA

M. Clearwater
Horticulture and Food Research Institute of New Zealand, Te Puke Research Center, Te Puke, New Zealand

P. Campanello
Laboratorio de Ecología Funcional, Departamento de Biología, FCEN, Universidad de Buenos Aires, Buenos Aires, Argentina

Present address:
G. Goldstein · T. Jones, Department of Biology, University of Miami, Coral Gables, FL 33124, USA

Introduction

Development of the concept of hydraulic architecture by Zimmermann (1978, 1983) has led to numerous studies of

the structure and properties of the water transport system of trees that govern the balance between efficiency of water supply and total transpiring leaf area (e.g. Ewers and Zimmermann 1984; Tyree et al. 1991). The xylem water transport property most often characterized is hydraulic conductivity, which is typically normalized by xylem cross-sectional area or by the total leaf area distal to the segment in which hydraulic conductivity has been measured (Tyree and Ewers 1991). Vulnerability of xylem to cavitation is often determined concurrently with hydraulic properties (Tyree et al. 1991; Cochard et al. 1997). Previously, most studies of hydraulic architecture have focused on the locations of major hydraulic constrictions in the branching system, and on variation in leaf area-specific conductivity associated with branching hierarchy (Salleo et al. 1982; Ewers and Zimmermann 1984; Ewers et al. 1989). Recently, however, more detailed information on axial and radial variation in xylem hydraulic properties in the stems of large trees has become available (Domec and Gartner 2001, 2002; Spicer and Gartner 2001). Although spatial variation in xylem structure and hydraulic architecture should exert a strong influence on axial and radial patterns of water movement in intact trees, we know of no published studies in which patterns of water movement in vivo and corresponding xylem properties at the same locations have been compared in the same individuals.

Most of the rapidly expanding literature on water movement in intact trees has emphasized the use of sap flow techniques such as thermal dissipation to make estimates of whole-tree water use (e.g. Wullschleger et al. 1998). Because sap flow is typically measured over a relatively narrow range of sapwood depth, usually close to the vascular cambium where flow is often, but not always, near maximal, the reliability of scaling from these measurements to whole-tree water use is constrained by uncertainty about radial profiles of sap flow, particularly in large trees with deep sapwood. Consequently, the spatial resolution of sap flow measurements is usually not adequate for comparison with detailed measurements of spatial variation in xylem water transport properties in trees with thick sapwood. The recent development of a modified heat dissipation probe that allows measurements of sap flow over small radial increments and a broad range of sapwood depth (James et al. 2002) should facilitate detailed comparisons of spatial variation in xylem structure and hydraulic properties with actual patterns of water flow observed in vivo. However, the heat dissipation technique provides estimates of sap flux density, which, even though it can be expressed in units consistent with velocity, is not a true sap velocity because it represents mass or volume flow normalized by total cross-sectional area of the conducting xylem rather than lumen area. Sap flux density expressed in velocity units is thus expected to severely underestimate maximum sap velocity in the largest conducting elements. On the other hand, injection of tracers such as deuterated water into the transpiration stream can provide absolute and independent estimates of maximum sap velocity based on the total path length traversed and the time elapsed between injection of the tracer at the base of the tree and its arrival in the uppermost leaves.

Ideally, spatial variation in sap flow would be consistent with variation in xylem hydraulic properties at the same locations. However, phenomena such as capacitance may partially confound direct comparisons of water flow in vivo with hydraulic properties determined in excised tissue. Hydraulic properties of xylem segments are usually determined from quasi steady-state flows generated by a constant driving force, whereas steady state flows and driving forces rarely prevail in intact trees during periods of rapid and fluctuating transpiration. Capacitive exchange of water between storage compartments and the transpiration stream will introduce a lag between variations in transpiration and variations in sap flow and will increasingly dampen variations in the driving force for water movement as the base of the tree is approached. The magnitude of this lag, and therefore the duration of non-steady state flow, generally increases with tree size and with increasing distance from the crown (Phillips et al. 1997; Goldstein et al. 1998). Thus, even if xylem hydraulic properties were identical near the ground and at the base of the crown in a large tree, it is likely that corresponding patterns of sap flow would differ.

The aims of this study were to (1) employ both heat and stable isotope tracers to characterize radial and axial patterns of water movement in tropical forest canopy trees with deep sapwood, and (2) relate patterns of water movement to xylem hydraulic properties inferred from vessel anatomical characteristics, and to other features such as tree size and relative diurnal water storage capacity. Specially constructed thermal dissipation probes (Granier 1985; James et al. 2002) were used to continuously monitor the rate of heat removal by flowing sap, and the distribution of deuterated water was monitored at intervals after its injection into the bases of the trees.

Materials and methods

Field site and plant material

The study was carried out in a seasonally dry tropical forest in the Parque Natural Metropolitano, Panama City, Republic of Panama (09°10'N, 79°51'E, elevation 50 m), at the site of the Smithsonian Tropical Research Institute canopy crane. The mean annual rainfall at the site is about 1,800 mm, of which less than 150 mm normally falls during the dry season between January and April. Single individuals of *Anacardium excelsum* (Bentero & Balb. ex Kunth) Skeels (Anacardiaceae), *Cordia alliodora* (R. & P.) Oken. (Boraginaceae), *Ficus insipida* Willd. (Moraceae), and *Schefflera morototoni* (Aubl.) Maguire, Steyerm. & Frodin (Araliaceae) were studied during the dry seasons (February–April) of 2000 and 2001 (Table 1). *F. insipida* and *S. morototoni* are evergreen, *A. excelsum* is brevideciduous and rapidly renews all of its leaves early in the dry season, and *C. alliodora* is gradually deciduous with peak leaf fall occurring between April and June. The crane's gondola was used to gain access to the crowns and upper trunks of the study trees.

Table 1 Characteristics of the trees studied at the Parque Natural Metropolitano, Panama canopy crane site. Diameter and sapwood area were measured at the height of the lowest set of sap flow probes (1.3–3.5 m). Values of whole-tree water use are means and standard error of 56–66 days of measurement. Sap flux density was calculated from water-use and sapwood area values

Species	Diameter (m)	Height (m)	Basal sapwood area (m^2)	Water use (kg day^{-1})	Sap flux density (g cm^{-2} day^{-1})	D_2O injected (ml)
Anacardium excelsum	0.98	38	0.66	750±11	114	120
Ficus insipida	0.65	28	0.31	331±3	107	125
Schefflera morototoni	0.47	22	0.15	108±3	72	65
Cordia alliodora	0.34	26	0.07	46±1	66	45

Water transport measured by heat dissipation sensors

Variable length heat dissipation sap flow probes with a heated and reference sensor measuring length of 10 mm at the probe tip (James et al. 2002) were used to determine sap flux density at different radial depths and vertical positions in the four trees. At the base of each tree, two replicate sets of probes were installed on opposite sides of the trunk. Sensors were inserted at five depths in the lower trunk at a height of 3.1 m for *A. excelsum* (5–23 cm), 3.5 m for *F. insipida* (4–24 cm) and 1.5 m for *S. morototoni* (1–18 cm), and at four depths 1.5 m high for *C. alliodora* (2–11 cm). The canopy crane was used to install two additional series of three to five probes in the upper trunk near the base of the crown at a height of 21 m for *A. excelsum* (2.5–18.5 cm), 16.3 m for *C. alliodora* (1.7–7 cm), and 12.8 m for *S. morototoni* (2–10 cm). Probes were not installed in the upper trunk of *F. insipida*.

For probe installation, two 2.58-mm-diameter holes, separated vertically by 10 cm, were drilled into the sapwood. The pairs of sensors at the base of the trunk were placed in an upward spiral around the tree, 10 cm apart vertically and 5 cm apart circumferentially at successive depths. In addition, a single pair of sensors was installed at a sapwood depth of approximately 1.3 cm in each of three (2001) or five (2000) replicate branches in the upper crown (branch diameter about 5 cm). The sensors were coated with thermally conductive silicone heat sink compound prior to insertion. All probes were protected from direct sunlight and rainfall by reflective insulation. Concurrent differential voltage measurements across the copper thermocouple leads were converted to a temperature difference between the heated and reference sensor (ΔT). Signals from the sap flow probes were scanned every minute and 10 min means were recorded by a data logger (CR10x or CR21x; Campbell Scientific, Logan, Utah) equipped with a 32-channel multiplexer (AM416; Campbell Scientific) and stored in a solid-state storage module (SM192; Campbell Scientific).

The temperature difference between the two probes (ΔT) was converted to sap flux density (v; g m^{-2} s^{-1}) using the calibration of Granier (1985):

$$v = 119k^{1.231}$$

where

$$k = (\Delta T_m - \Delta T)/\Delta T$$

and where ΔT_m is the temperature difference when sap flux density is assumed to be zero. The mass flow of sap corresponding to each trunk probe (F; g s^{-1}) was calculated as:$F=vA$ where A (m^2) is the cross-sectional area of the sapwood calculated as the ring area centered on the 10-mm-long sensor and extending to midway between two sensors of successive depth. The innermost sensor was considered to measure the sap flux density to the estimated depth of heartwood. Sapwood area was calculated with the assumption of radial symmetry.

Whole-tree daily water use (kg day^{-1}), calculated from radial profiles of sap flow near the base of the tree, was assumed to be equal to total daily transpiration. The time course of branch sap flow was used as a surrogate for the time course of whole-crown transpiration. For each 10-min measurement, the average sap flow of three to five branches was calculated and divided by the daily maximum value to obtain an estimate of normalized whole-crown transpiration. Sap flow measured at the two outermost depths near the base of the trunk was normalized in a similar manner. The effect of stem water storage on diurnal patterns of sap flow was assessed by subtracting the daily course of normalized flow near the base of the tree from the daily course of normalized crown sap flow (Goldstein et al. 1998). Positive values of crown minus basal sap flow indicate that water is being withdrawn from storage compartments located between the upper branches and the base of the trunk. Larger maximum values of normalized crown minus basal sap flow reflect greater relative reliance on withdrawal of water from internal storage compartments to transiently replace transpirational losses during the morning when transpiration is increasing.

Xylem anatomical analyses

Wood samples were collected from the same individuals of *A. excelsum*, *C. alliodora*, *F. insipida* and *S. morototoni* in which sap flow was measured. Cores to the center of the stem, or as deep as possible, were collected using a 5-mm-diameter increment borer at sites corresponding to the placement of sap flow sensors in the upper and lower trunk, and upper branches. Samples were placed in fixative (10% formaldehyde, pH 8.0) and stored at 5°C. Segments of 10-mm length were taken from the cores at the position corresponding to the placement of the sensitive portion of the sap flow sensors. Two segments of 5 mm were sectioned separately and the data combined. Transverse sections of 55-μm thickness were made using a freezing cryotome (Cryocut 1800, Reichert-Jung) and mounted in frozen tissue embedding medium (HistoPrep, Fisher Scientific, Fairlawn, N.J.). Sections were photographed at ×25 magnification in three representative regions. Cross-sections of petioles of *S. morototoni* and terminal branchlets of *A. excelsum* and *C. alliodora* were also analyzed. Vessel dimensions were determined using SigmaScan Pro 4 (SPSS, Chicago, Ill.). After calibrating the digitized photomicrographs, the perimeter of the vessels was outlined, and the lumen area was determined. The lumen diameter of each entire vessel within the image was calculated assuming the lumen to be circular. The area occupied by vessel lumens as a proportion of the image area (wood area) was calculated. The number of vessels per mm^2 (vessel density) was computed using the average between the total number of vessels (entire and partial) and the number of entire vessels for each image. To eliminate vessels that may have been tapering, only those vessels having a lumen diameter of greater than half the diameter of the largest vessel were included in calculations of average vessel lumen diameter for each wood segment.

Theoretical specific conductivity of the wood in the upper trunk was calculated according to the equation for capillaries:

$$k_s = \frac{\pi\rho}{128\eta A_{image}} \sum_{i=1}^{n} d_i^4 \quad (3)$$

where k_s is theoretical wood specific conductivity (kg m^{-1} MPa^{-1} s^{-1}), A_{image} is the area of the images; ρ is the density of water at 27°C (kg m^{-3}); η is the dynamic viscosity of water (MPa s); and d_i are the diameters of single vessels summed over the number of vessels, n, per unit cross-sectional area.

The vessel path-length from the base of the tree to the position of collection for each of the wood cores was determined

trigonometrically from the vertical height of the point of collection, the horizontal distance from the base of the tree and, in most cases, a mid-point vertical height determination.

Tracing D_2O in transpired water and xylem tissues

Deuterium oxide (99.9 atom % D D_2O, Aldrich Chemical, Milwaukee, Wis.) was injected into the base of the four trees to assess the rate of xylem sap flow to the crown, the relative magnitude of exchange of water between the transpiration stream and storage compartments within the trunk and branches, and the relative magnitude and extent of radial water movement. The total volume of D_2O injected into each tree was determined according to the volume of D_2O per trunk diameter injected into *Eucalyptus grandis* by Dye et al. (1992) and Kalma et al. (1998) (Table 1). Holes (5-mm diameter, 50-mm deep) were drilled at an angle of 30° from horizontal down and into the trunk, 30–40 cm above ground level at 4–6 cm intervals around the circumference of the trunk. The volume of D_2O was evenly distributed between the holes. For *F. insipida*, D_2O was injected 30 cm above the ground at the base of the trunk and extending along the buttress roots. D_2O was injected into the trunk immediately after drilling and the holes were sealed with wood putty. Injections were initiated and completed between 0900 and 1100 hours. Continuous monitoring of sap flux density indicated that it was not noticeably affected by the process of D_2O injection.

Presence of the D_2O tracer in transpired water was detected by collecting five leaves from different regions of the crown, which were sealed within clear plastic bags and left in direct sunlight for about 30 min. Approximately 30 µl of condensed water was then collected with a 100-µl micropipette capillary and the ends were rapidly sealed with a gas torch. The baseline D_2O signal in transpired water was determined by collecting samples of transpired water for 4 days prior to D_2O injection. After the injection of D_2O (day 0), transpired water was collected daily for 10 days, with additional collections up to 27 days after injection. In all cases, leaves were collected at 1200 hours.

Xylem tissue samples were collected from all four trees to assess the vertical and radial movement of D_2O during the measurement period. Samples were collected 1 day prior to injection, and on post-injection days 1 and 8. Two 5-mm-diameter wood cylinders were obtained using an increment borer at each of three heights (breast height, upper trunk, and upper crown). The total core length was approximately the radius of the stem, and wood segments of 2–6 cm were immediately placed in a glass vial, sealed with a rubber stopper and Parafilm, and stored at 0°C to prevent evaporative fractionation. Water was extracted from the xylem by cryogenic vacuum distillation.

All transpired water and xylem samples were sent to Mountain Mass Spectrometry (Evergreen, Colo.) for preparation and analysis. Hydrogen gas for isotopic analysis was generated from 4 µl subsamples by the zinc reduction method (Coleman et al. 1982). The stable hydrogen isotope composition of the water samples was expressed in conventional delta (δ) notation as the D/H ratio relative to a V-SMOW standard as:

$$\delta = \left[\left(\mathrm{D/H_{sample}} - \mathrm{D/H_{standard}}\right) - 1\right] \times 1{,}000 \quad (4)$$

δD values of transpired water were normalized with respect to the maximum value for each tree to facilitate comparison of the time courses of detection and disappearance of the D_2O signal in transpired water. For each transpired and xylem water sample, two subsamples were analyzed and an average value was calculated. The velocity of D_2O transport was estimated as the tree height divided by the number of days required to detect the D_2O tracer in transpired water. The residence time of the D_2O signal was taken as the time elapsed between detection of the maximum signal in transpired water and its return to baseline levels prior to injection. Movement of the tracer was also compared by normalizing transpired water and xylem water δD values relative to the mean soil water δD value between 20 cm and 1 m depth (–52.7‰), previously measured at the site during the dry season (Andrade, Goldstein and Meinzer, unpublished data).

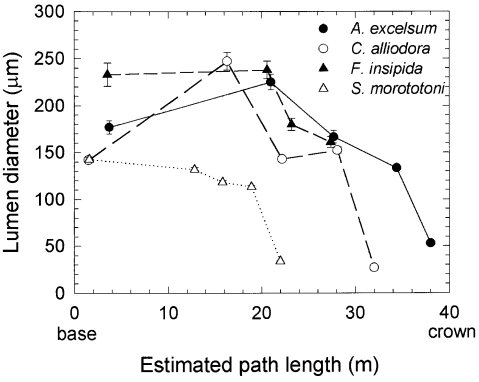

Fig. 1 Relationship between vessel lumen diameter in the outermost 1.7 cm of sapwood and estimated xylem path length from the base of the tree to the crown for *Anacardium excelsum*, *Cordia alliodora*, *Ficus insipida*, and *Schefflera morototoni*. For each species, the second symbol from the left represents the upper trunk near the base of the crown

Results and discussion

Xylem anatomy

Sapwood anatomical characteristics varied axially and radially within and among trees. Vessel lumen diameter increased axially from the upper crown to the upper trunk near the base of the crown in each of the four trees (Fig. 1). Vessel diameters have also been found to increase from the petioles to the roots in temperate tree species (Zimmermann 1978, 1983; Gartner 1995). West et al. (1999) hypothesized that the total hydraulic resistance of trees would be independent of path length if the taper of xylem elements between successive segments from the petioles to the base of the tree exceeds a critical value. Becker et al. (2000) subsequently concluded that partial buffering of hydraulic resistance from path-length effects could occur even when tapering does not exceed the threshold value derived by West et al. (1999). Although axial trends in vessel lumen diameter in the crowns of the four study trees appeared to be consistent with partial buffering of hydraulic resistance from path-length effects, lumen diameter remained relatively constant from the upper to lower trunk (Fig. 1). The dependence of total hydraulic resistance on path length among the four study trees is uncertain because resistance is dependent on vessel density as well as vessel lumen diameter, and increased sapwood cross-sectional area toward the base of the tree may have compensated for the nearly constant vessel diameter along the trunk.

The trunks of four study species had large vessels with diameters ranging from 100 to 250 µm, which contributed to low vessel densities (Fig. 2). Vessel diameters in the trunks of the four study trees exceeded those of many co-occurring liana species (Ewers et al. 1997). However, the

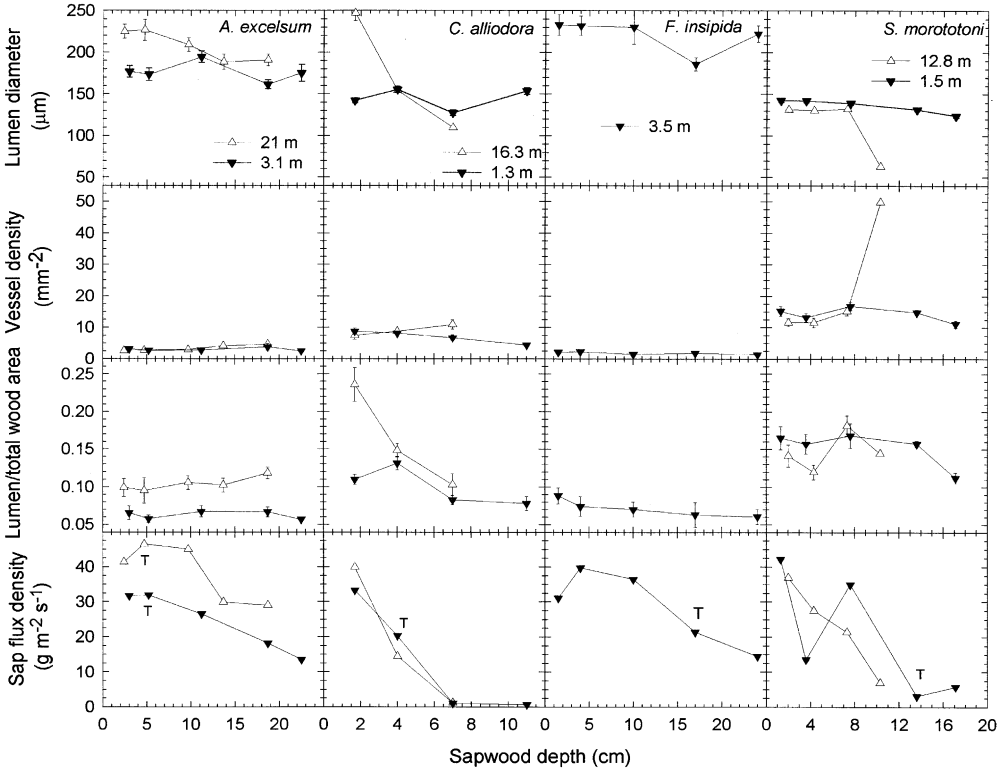

Fig. 2 Vessel lumen diameter (μm), vessel density (mm^{-2}), lumen area per wood area and sap flux density ($g\ m^{-2}\ s^{-1}$) with radial sapwood depth within the lower and upper trunk for *A. excelsum*, *C. alliodora*, *F. insipida*, and *S. morototoni*. *Vertical bars* represent standard errors, which in some cases are smaller then the symbol. The depth at which tyloses were first observed within vessels has been indicated in the sap flux density panel (*T*). Sap flux density is the average sap flux density for 10-min measurements from 1000 to 1400 hours for 56–66 days during the 2000 or 2001 dry season at the Smithsonian canopy crane site in Parque Natural Metropolitano, Panama

proportion of lumen area generally did not exceed 20% of cross-sectional area, which is in the range (6–55%) documented for a number of woody species (Gartner 1995). Whereas xylem elements typically become longer and wider, and decline in density, with an increase in cambial age or diameter of the stem (Gartner 1995; Mencuccini et al. 1997), no pronounced radial trends in vessel diameter were observed among the four tropical forest canopy trees studied here with the exception of the upper trunk of *C. alliodora* and *S. morototoni* (Fig. 2).

Spatial variation in sap flow

Sap flux density decreased from the outermost to innermost sapwood in all four study trees (Fig. 2). Three distinct types of radial profiles were observed. In the upper and lower trunk of *C. alliodora* and in the upper trunk of *S. morototoni*, a sharp, nearly linear decrease in sap flow with increasing sapwood depth occurred. In contrast, sap flow initially increased then decreased slowly with increasing sapwood depth in *A. excelsum* and *F. insipida*. In both of these species, substantial rates of sap flow were measured at sapwood depths greater than 20 cm. Technical constraints prevented installation of probes at greater depths. The third type of radial profile, which was observed only near the base of the trunk of *S. morototoni*, consisted of sharp, alternating decreases and increases in flow with increasing sapwood depth. There were no consistent axial trends in maximum sap flux

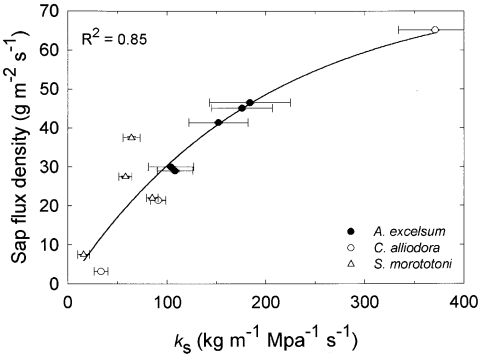

Fig. 3 Relationship between calculated specific conductivity of xylem within the upper trunk, and the sap flux density at corresponding depths

density or radial flow profiles among the three trees with sets of probes installed in both the lower and upper trunk.

Axial and radial variation in sap flow did not appear to be closely related to variation in individual sapwood anatomical characteristics such as vessel diameter, vessel density, or the proportion of lumen area in relation to total xylem cross-sectional area determined from samples collected near the sap flow measurement locations (Fig. 2). However, radial variation in sap flux density in the upper trunk of *A. excelsum*, *C. alliodora*, and *S. morototoni* was strongly correlated with corresponding values of maximum k_s calculated for each sensor location (Fig. 3). At a given predicted k_s, sap flux density was similar for the three species regardless of differences in

tree size and architecture. The tendency for sap flux density to saturate with increasing k_s, indicates factors other than k_s began to limit maximum rates of flow. The most likely explanation for the pattern in Fig. 3 is the dependence of flow on both the driving force for water movement and k_s. At a given soil-to-leaf water potential difference (driving force), regions of sapwood with greater k_s would experience smaller axial tension gradients, which would diminish the response of sap flow to increasing k_s. This explanation raises the possibility of radial tension gradients in large stems, which could induce substantial radial water movement if the radial hydraulic connections between adjacent layers of sapwood are good. Although the sap flow probe design employed would presumably detect radial water movement via cooling of the heated sensor, it did not permit partitioning of flow into radial and axial components.

Axial and radial transport of D_2O

Deuterium enrichment was first detected in transpired water after a single day for *C. alliodora*, 2 days for *F. insipida*, 3 days for the larger *A. excelsum*, and after 5 days for *S. morototoni* (Fig. 4). The times required for the arrival of D_2O from the base of the tree to the crown in the present study were similar to those reported from other studies in which deuterium was used as a tracer for a range of tree sizes (Dye et al. 1992; Kalma et al. 1998). The rate of transport of D_2O from the tree base to the crown, or the maximum sap velocity, was calculated to range from approximately 0.5 m h^{-1} for *S. morototoni* to 1.9 m h^{-1} for *C. alliodora*. Because these estimates include the entire daily cycle, maximum sap velocities during the daylight hours are expected to be substantially higher. In *C. alliodora*, for example, maximum sap velocity was probably greater than 4 m h^{-1} because substantial flow occurred during less than 12 h of the 24 h required for the tracer to be detected in the crown. It is important to note that total path length did not appear to be the major determinant of the time elapsed before D_2O was detected in transpired water, because tracer arrival times ranged from 1 to 5 days among three of the trees with a height range of only 22–28 m (Table 1). Sap flux density expressed in velocity units invariably yielded unrealistically low estimates of maximum sap velocity. Mean maximum sap flux density was about 40 g m^{-2} s^{-1}, which is only 0.14 m h^{-1} in velocity units.

Variation in the time required for δD values of transpired water to return to background levels, was even greater than the variation in arrival times (Fig. 4). In *C. alliodora*, for example, δD values of transpired water had declined sharply from their maximum to the baseline only 2 days after maximum amounts of tracer were recorded, whereas in *A. excelsum* 22 days elapsed before δD values were indistinguishable from background levels. Patterns of transport and retention of the D_2O tracer along an axial gradient from the base of the trunk to the leaves are shown in Fig. 5. As expected, the tracer was detected in

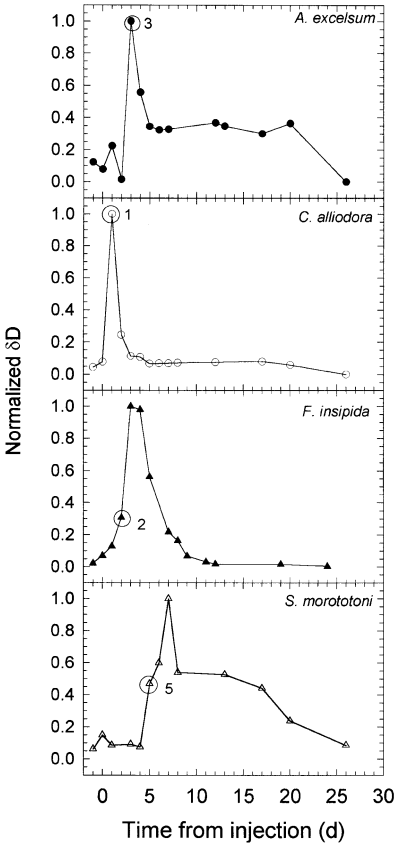

Fig. 4 Time course of normalized δD from pre-injection to 26 days after the injection of D_2O 30 cm above soil level into *A. excelsum*, *C. alliodora*, *F. insipida* and *S. morototoni* at the Smithsonian canopy crane site in Parque Natural Metropolitano, Panama. Day 0 is the day of injection, and the day of detection of D_2O in the upper crown is indicated with the *day number* and a *circle*

xylem sap near the base of the trunk of all four trees on the day following injection. In *C. alliodora* the tracer had already appeared in all portions of the tree sampled, but was not yet detectable in the upper trunk, branches and leaves of the remaining trees. By 8 days after injection, however, the tracer was undetectable in all portions of the *C. alliodora* tree sampled, but was still detectable in portions of the other three trees. Evidence of radial transport of D_2O was found in the lower trunk of *A. excelsum*, *F. insipida* and *S. morototoni* 1 day after injection (Table 2). In *A. excelsum*, the tracer had penetrated to a depth of at least 14.7 cm, *F. insipida* to a depth of at least 17.4 cm, and in *S. morototoni* to a radial depth of greater than 21.8 cm. In *C. alliodora*, there was no consistent evidence that the tracer had penetrated further than the 5 cm depth of injection. At 8 days after injection, the tracer was still evident at all radial depths sampled in *S. morototoni*. The transport of D_2O within the sapwood of the Panamanian tree species studied here followed a pattern similar to that of *E. grandis* in which substantial diffusion of D_2O through the rays and axial parenchyma into the heartwood was observed regardless

Table 2 Radial xylem sap δD values from wood samples taken at 1.3 m height prior to, and after injection of D_2O

Species	Xylem depth (cm)	Xylem sap δD (‰)		
		–1 day	1 day	8 days
Anacardium excelsum	4.7	–39.7	166	38.3
	9.5	–54.3	–37.1	–47.8
	14.7	–49.7	–33.2	–53.2
	22.7	–44.6	–44.1	–49.9
Ficus insipida	4.8	–40.4	44.8	–33.6
	9.6	–45.7	–20.3	–34.9
	13.9	–38.9	–26.5	–37.8
	17.4	–33.9	–26.8	–34.2
Schefflera morototoni	4.8	–42.6	3,391	479
	9.6	–47.3	95.4	20.5
	14.0	–52.6	45.2	–
	21.8	–53.0	–13.2	–39.1
Cordia alliodora	5.0	–44.9	95.9	–40.7
	9.7	–35.4	–43.0	–39.3
	14.3	–48.8	–35.8	–43.3
	18.9	–	–53.7	–58.8

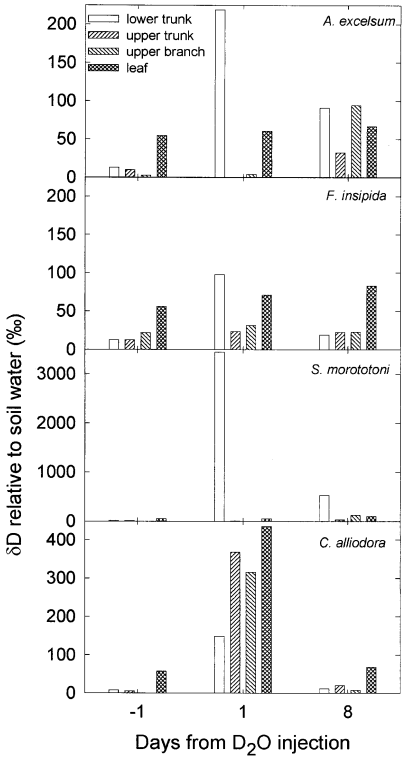

Fig. 5 δD of xylem water relative to soil water in the outermost sapwood in the lower trunk, upper trunk, a branch in the crown and in transpired leaf water prior to, and after the injection of D_2O

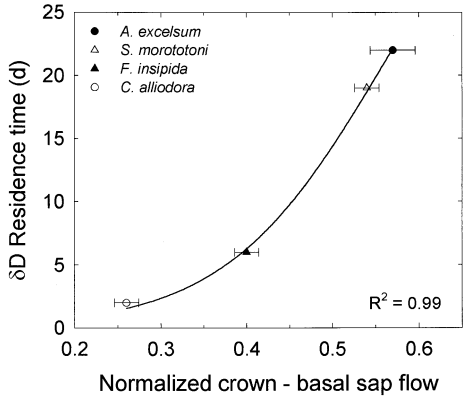

Fig. 6 The residence time of the δD signal within transpired water for the four study species in relation to the maximum difference between crown and basal sap flow while transpiration was increasing during the morning

of whether the D_2O was injected into sapwood or both sapwood and heartwood. (Kalma et al. 1998).

Taken together, the preceding results suggest that capacitive exchange of water between the transpiration stream and storage compartments in the stem played a major role in determining the persistence of the D_2O tracer in the xylem sap. Both the residence time and radial transport of the tracer can be hypothesized to be greater in trees with greater relative diurnal water storage capacity. Consistent with this, a strong positive correlation was observed between the time required for δD values of transpired water to return to background levels and the maximum difference between crown and basal sap flow normalized with respect to their maximum values (Fig. 6). If sap flow in the branches of the upper crown is assumed to be a surrogate for transpiration, then lags between changes in sap flow in the crown and at the base of the tree reflect exchange of water between the transpiration stream and storage compartments located between the points at which sap flow is measured (Phillips et al. 1997; Goldstein et al. 1998). The maximum difference between crown and basal sap flow when transpiration is initially increasing during the morning hours can thus be used as an index of relative diurnal water storage capacity. Relative water storage capacity was highest in the largest tree (*A. excelsum*, 0.98-m diameter) and lowest in the smallest tree (*C. alliodora*, 0.34-m diameter), consistent with the findings of an earlier study conducted at the same site (Goldstein et al. 1998). However, it is not clear why

the 0.47-m-diameter *S. morototoni* tree appeared to have a greater relative diurnal water storage capacity than the larger 0.65-m-diameter *F. insipida* tree. Greater radial penetration of the tracer in *S. morototoni* than in *F. insipida* (Table 2) suggests that intrinsic differences in sapwood structure and radial transport properties may have contributed to the discrepancy between size and relative water storage capacity for these two trees. Although a linear regression would have yielded an adequate fit to the data in Fig. 6, the sigmoid function selected has a sounder physical basis. The *y*-intercept is constrained by the requirement for minimum δD residence times to be greater than zero, and maximum residence times are constrained by the limit of 1.0 for normalized crown minus basal sap flow. If the relationship in Fig. 6 holds for a larger number of tree species, the residence time of a tracer could be used as a predictor of relative internal water storage capacity.

The velocity of D_2O tracer transport from the base of the tree to the crown was positively correlated with both the maximum theoretical k_s of the outer sapwood in the upper trunk and the ratio of tree height to normalized crown minus basal sap flow (Fig. 7). The latter is an index of distance traveled in relation to the capacity for exchange of water between storage compartments and the transpiration stream. The velocity of D_2O transport to the crown was highest in *C. alliodora*, which had the lowest relative water exchange capacity in relation to its height and largest theoretical k_s of the four trees. *S. morototoni*, by contrast, had the highest relative water exchange capacity in relation to its height, lowest theoretical k_s, and slowest axial transport of D_2O. Although linear regressions provided good fits to the data in Fig. 7 over the ranges of the variables observed, it is reasonable to expect that the relationship between k_s and tracer velocity should intersect with the origin and that tracer velocity should asymptotically approach zero as the ratio of tree height to relative water exchange capacity decreases further. When maximum sap velocity was estimated by normalizing sap flux density by the ratio of vessel lumen area to xylem cross-sectional area to account for non-conducting xylem, no universal relationship between sap velocity and tracer velocity was obtained. A highly significant linear correlation (r^2=0.99) between estimated sap velocity and D_2O velocity was obtained for *A. excelsum*, *F. insipida* and *S. morototoni*, but *C. alliodora* appeared as an outlier. The inverse relationship between k_s and the ratio of internal water exchange capacity to path length (tree height) evident in Fig. 7 suggests a possible trade-off that may contribute to relative homeostasis of leaf water status through highly efficient water transport at one extreme and buffering of diurnal fluctuations in leaf water status via release of stored water at the other extreme.

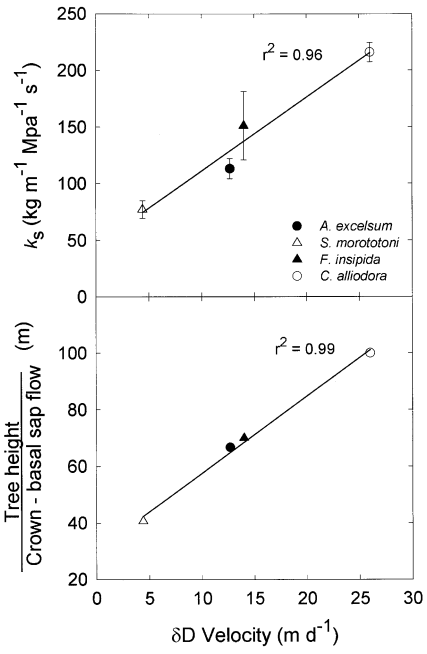

Fig. 7 Rate of transport of the D_2O tracer within xylem water of the four study species in relation to the theoretical maximum specific conductivity of outer sapwood in the upper trunk, and the ratio of tree height to normalized crown-basal sap flow, an index of distance traveled in relation to relative diurnal water storage capacity

Conclusions

The magnitude of radial variation in sap flow observed here and the thickness of sapwood over which it occurred point to the difficulty of estimating whole-tree water use from measurements of sap flow over a limited range of sapwood depth at few locations. Marked radial and axial variation in water transport characteristics, xylem anatomy and xylem hydraulic properties among the four co-occurring species studied obscured common features shared by all of the species. These features included the dependence of sap flux density on xylem hydraulic properties, the dependence of D_2O tracer velocity (an estimate of maximum sap velocity) on xylem hydraulic properties, the dependence of tracer velocity on the distance traveled in relation to tree internal water exchange capacity, and the dependence of tracer residence time on diurnal water exchange capacity. Capacitive exchange of water between stem storage compartments and the transpiration stream thus had a profound influence on apparent rates of axial water transport, the magnitude of radial water movement, and the retention time in the tree of water taken up by the roots. Transport velocities of chemical signals in the transpiration stream may be constrained in a similar manner by water storage characteristics, unless they are actively sequestered by living cells imbedded in the xylem. Capacitance is thus a component of hydraulic architecture that needs to be taken into account in predicting and interpreting patterns of water movement

in intact trees. Our findings suggest that in addition to the possibility that total water transport may scale universally with tree size (Enquist et al. 1998; Meinzer et al. 2001), water movement within trees may be governed in a universal manner by features of hydraulic architecture operating at multiple scales.

Acknowledgements This research was supported by National Science Foundation Grants IBN 94–19500 and IBN 99–05012. We thank the Smithsonian Tropical Research Institute for providing facilities and logistical support, and the expertise of the Smithsonian canopy crane operators. We are also grateful to B. Hines and N. Olivo for their able assistance in the field.

References

Becker P, Gribben RJ, Lim CM (2000) Tapered conduits can buffer hydraulic conductance from path-length effects. Tree Physiol 20:965–967

Cochard H, Peiffer M, Le Gall K, Granier A (1997) Developmental control of xylem hydraulic resistances and vulnerability to embolism in *Fraxinus excelsior* L.: impacts on water relations. J Exp Bot 48:655–663

Coleman ML, Shepard TJ, Durham JJ, Rouse JE, Moore GR (1982) Reduction of water with zinc for hydrogen isotope analysis. Anal Chem 54:993–995

Domec J-C, Gartner BL (2001) Cavitation and water storage capacity in bole xylem segments of mature and young Douglas-fir trees. Trees 15:204–214

Domec J-C, Gartner BL (2002) Age- and position-related changes in hydraulic versus mechanical dysfunction in xylem: inferring the design criteria for Douglas-fir wood structure. Tree Physiol 22:91–104

Dye PJ, Olbrich BW, Calder IR (1992) A comparison of the heat pulse method and deuterium tracing method for measuring transpiration from *Eucalyptus grandis* trees. J Exp Bot 43:337–343

Enquist BJ, Brown JH, West GB (1998) Allometric scaling of plant energetics and population density. Nature 395:163–165

Ewers FW, Zimmermann MH (1984) The hydraulic architecture of eastern hemlock (*Tsuga canadensis*). Can J Bot 62:940–946

Ewers FW, Fisher JB, Chiu ST (1989) Water transport in the liana *Bauhinia fassoglensis* (Fabaceae). Plant Physiol 91:1625–1631

Ewers FW, Carlton MR, Fisher JB, Kolb KJ, Tyree MT (1997) Vessel diameters in roots versus stems of tropical lianas and other growth forms. IAWA J 18:261–279

Gartner BL (1995) Patterns of xylem variation within a tree and their hydraulic and mechanical consequences. In: Gartner BL (ed) Plant stems: physiology and functional morphology. Academic Press, San Diego, pp 125–149

Goldstein G, Andrade JL, Meinzer FC, Holbrook NM, Cavelier J, Jackson P, Celis A (1998) Stem water storage and diurnal patterns of water use in tropical forest canopy trees. Plant Cell Environ 21:397–406

Granier A (1985) Une nouvelle méthode pour la mesure du flux de sève brute dans le tronc des arbres. Ann Sci For 42:193–200

James SA, Clearwater MJ, Meinzer FC, Goldstein G (2002) Variable length heat dissipation sensors for the measurement of sap flow in trees with deep sapwood. Tree Physiol 22:277–283

Kalma SJ, Thorburn PJ, Dunn GM (1998) A comparison of heat pulse and deuterium tracing techniques for estimating sap flow in *Eucalyptus grandis* trees. Tree Physiol 18:697–705

Meinzer FC, Goldstein G, Andrade JL (2001) Regulation of water flux through tropical forest canopy trees: do universal rules apply? Tree Physiol 21:19–26

Mencuccini M, Grace J, Fiorvanti M (1997) Biomechanical and hydraulic determinants of tree structure in Scots pine: anatomical characteristics. Tree Physiol 17:105–113

Phillips N, Nagchaudhuri A, Oren R, Katul G (1997) Time constant for water transport in loblolly pine trees estimated from time series of evaporative demand and stem sapflow. Trees 11:412–419

Salleo S, Rosso R, Lo Gullo MA (1982) Hydraulic architecture of *Vitis vinifera* L. and *Populus deltiodes* Bartr. 1-year-old twigs. I. Hydraulic conductivity (LSC) and water potential gradients. G Bot Ital 116:15–27

Spicer R, Gartner BL (2001) The effects of cambial age and position within the stem on specific conductivity of Douglas-fir (*Pseudotsuga menziesii*) sapwood. Trees 15:222–229

Tyree MT, Ewers FW (1991) The hydraulic architecture of trees and other woody plants. New Phytol 119:345–360

Tyree MT, Snyderman DA, Wilmot TR, Machado JL (1991) Water relations and hydraulic architecture of a tropical tree (*Schefflera morototoni*). Tree Physiol 96:1105–1113

West GB, Brown J, Enquist BJ (1999) A general model for the structure and allometry of plant vascular systems. Nature 400:664–667

Wullschleger SD, Meinzer FC, Vertessy RA (1998) A review of whole-plant water use studies in trees. Tree Physiol 18:499–512

Zimmermann MH (1978) Hydraulic architecture of some diffuse-porous trees. Can J Bot 56:2286–2295

Zimmermann MH (1983) Xylem structure and the ascent of sap. Springer, Berlin Heidelberg New York